[Applications and Applied Mathematics: An International Journal (AAM)](https://digitalcommons.pvamu.edu/aam)

Volume 10 | Issue 1 — Article 20

6-2015

Unsteady boundary layer flow of thermophoretic MHD nanofluid past a stretching sheet with space and time dependent internal heat source/sink

N. Sandeep
Gulbarga University

C. Sulochana
Gulbarga University

C. S. K. Raju
VIT University

M. J. Babu
VIT University

V. Sugunamma
Sri Venkateswara University

Available at
http://pvamu.edu/aam
Appl. Appl. Math.
ISSN: 1932-9466

Applications and Applied Mathematics:
An International Journal
(AAM)

Vol. 10, Issue 1 (June 2015), pp. 312-327

Unsteady boundary layer flow of thermophoretic MHD nanofluid past a stretching sheet with space and time dependent internal heat source/sink

N. Sandeep, C. Sulochana
Department of Mathematics
Gulbarga University
Gulbarga (K.A.) -585106, India
nsreddy.dr@gmail.com;
math.sulochana@gmail.com

C.S.K. Raju, M. Jayachandra Babu
Department of Mathematics
VIT University
Vellore (T.N.) - 632014, India
shivaphd90@gmail.com;
jayamacharla@gmail.com

V. Sugunamma
Department of Mathematics
Sri Venkateswara University
Tirupati (A.P.) -517502, India
vsugunar@gmail.com

Received: January 1, 2015; Accepted: March 10, 2015

Abstract

In this study we analyze the boundary layer flow of a thermophoretic magnetohydrodynamic dissipative nanofluid over an unsteady stretching sheet in a porous medium with space and time dependent internal heat source/sink. The governing equations are transformed to ordinary differential equations by using similarity transformation. Numerical solutions of these equations are obtained by using the Shooting Technique. The effects of non-dimensional governing parameters on the velocity, temperature, concentration profiles, friction factor, Nusselt and Sherwood numbers are discussed and presented through graphs and tables. Accuracy of the results compared with the existing ones. Excellent agreement is found with earlier studies.

Keywords: Boundary layer flow; MHD; Thermophoresis; Non-uniform source/sink; Dissipation; Stretching surface; Convection.

MSC 2010 No.: 34B15, 35Q35, 76R10, 76S05

1. Introduction

The development of nanotechnology is likely to bring unimaginable and multi-dimensional changes in our way of life, in the coming years. Recently many researchers focused on this topic due to its prominent importance in engineering and allied areas. Heat and mass transfer of thermophoretic magnetohydrodynamic flow has potential applications like air cleaning, aerosol particles sampling, nuclear reactor safety, micro electronics manufacturing etc. The detailed analysis on thermophoretic flows was discussed by Derjaguin and Yalamov (1965). The boundary layer flow of thermophoresis of aerosol particles over vertical flat plate was analyzed by Goren (1977). The term "nanofluid" was first introduced by Choi (1995). He has given clear description about the heat transfer characteristics of nanofluids. Thermophoresis effect on aerosol particle deposition over a flat plate was analyzed by Tsai (1999). Chamka and Issa (2000) analyzed the heat and mass transfer of MHD thermophoretic flow over flat surface.

A similarity analysis for boundary layer flow by applying transverse magneticfield was studied by Ece (2005). Chemical reaction and radiation effects on hiemenz flow in porous medium were studied by Seddeek et al. (2007). Radiation effect on mixed convection flow of micro polar fluid was discussed by Ibrahim et al. (2008). Phillip et al. (2008) discussed thermophysical properties and heat transfer characteristics of nanofluids. Afify (2009) proposed a similarity solution by considering suction/injection over stretching surface. The behavior of small sized particles over moving surface was presented by Bachok et al. (2009). Forced convective flow in rotating channel with conductive walls was presented by Seth et al. (2010). MHD visco-elastic flow over stretching sheet was analyzed by Prasad et al. (2010). Unsteady free convective magnetohydrodynamic flow over inclined porous plate was studied by Kabir and Mahbub (2012). Sandeep et al. (2012) discussed the effect of radiation and chemical reaction on transient MHD free convective flow through porous medium.

Thermophoretic MHD flow over isothermal vertical plate was studied by Noor et al. (2013). Yasin et al. (2013) discussed the volume fraction effects on three types of nanofluids namely Cu-water, Al_2O_3-water and TiO_2 and they concluded that the type of nanofluid is important to increase the heat transfer rate. Radiation effect on ethylene glycol based nanofluid over infinite vertical plate was studied by Sandeep et al. (2013). Magnetohydrodynamic flow over stretching sheet with slip effects was discussed by Rushikumar (2013). Effect of radiation by considering aligned magnetic field over flat plate was discussed by Manjulatha et al. (2014). Radiation and magnetic field effects on unsteady natural convection flow of a nanofluid past an infinite vertical plate with heat source was discussed by Mohan Krishna et al. (2014). They concluded that increase in volume fraction of nanoparticles decrease in velocity of the fluid. Uddin et al. (2014) proposed a model for MHD thermosolutal nanofluid with slip conditions in porous medium. Viscous dissipation and chemical reaction effects on MHD free convective flow through porous media was discussed by Dessie and Kishan (2014). Ghalambaz and Noghrehabadi (2014) studied heat and mass transfer characteristics of nanofluid over a vertical plate in porous medium.

To the authors' knowledge no studies have been reported on the boundary layer flow of a thermophoretic MHD dissipative nanofluid over an unsteady stretching sheet in a porous medium by considering space and time dependent internal heat source/sink (nonuniform heat source/sink). In this study the governing equations are transformed to ordinary differential equations by using similarity transformation. Numerical solutions of these equations are obtained by using the Shooting Technique. The effects of non-dimensional governing parameters on the velocity, temperature, concentration profiles, friction factor, Nusselt and Sherwood numbers are discussed and presented through graphs and tables. Accuracy of the results to the existing ones and are found to be in excellent agreement with earlier studies.

2. Analysis of the flow

Consider an unsteady, incompressible, electrically conducting, two dimensional boundary layer flow of a dissipative nanofluid past a stretching sheet with non-uniform velocity $U_w(x,t)$ and permeability k'. The x-axis is along the continuous stretching surface and y axis is normal to the surface. An external magnetic field $B(x)$ is applied along the y direction. A non-uniform heat source/sink q''', suction/injection, thermophoresis effect along with volume fraction of nano particles is taken in to account. No slip occurs between suspended particles and base fluid. The boundary layer equations that govern the present flow subject to the Boussinesq approximations can be expressed as

$$\frac{\partial u}{\partial x}+\frac{\partial u}{\partial y}=0, \tag{1}$$

$$\frac{\partial u}{\partial t}+u\frac{\partial u}{\partial x}+v\frac{\partial u}{\partial y}=\upsilon\frac{\partial^2 u}{\partial y^2}-\frac{\sigma B^2}{\rho}u-\frac{\upsilon}{k'}u, \tag{2}$$

$$\frac{\partial T}{\partial t}+u\frac{\partial T}{\partial x}+v\frac{\partial T}{\partial y}=\alpha\frac{\partial^2 T}{\partial y^2}+\frac{\nu}{c_p}\left(\frac{\partial u}{\partial y}\right)^2+\tau\left(D_B\frac{\partial T}{\partial y}\frac{\partial C}{\partial y}+\frac{D_T}{T_\infty}\left(\frac{\partial T}{\partial y}\right)^2\right)+q''', \tag{3}$$

$$\frac{\partial C}{\partial t}+u\frac{\partial C}{\partial x}+v\frac{\partial C}{\partial y}=D_B\frac{\partial^2 C}{\partial y^2}+\frac{D_T}{T_\infty}\frac{\partial^2 T}{\partial y^2}, \tag{4}$$

where u and v are the velocity components in the x, y directions , υ is the kinematic viscosity, T and T_∞ are the temperatures of thermal boundary layer fluid and the free stream respectively, σ is the electrical conductivity , $B=B_0/\sqrt{1-ct}$ is the magnetic induction, $k'=k_0(1-ct)$ is the nonuniform permeability of the porous medium, α is the thermal diffusivity, ρ is the fluid density , c_p is the specific heat at constant pressure , q''' is the nonuniform heat source/sink , D_B is the Brownian diffusion coefficient and D_T is the thermophoretic diffusion coefficient.
The Boundary conditions for the model as follows

$$\begin{aligned}&u=U_w(x,t),\ v=V_w(x,t)\ ,\ T=T_w(x,t),\ C=C_w(x,t)\ \text{ at }\ y=0,\\&u=0,\quad T\to T_\infty\ ,\quad C\to C_\infty\quad \text{as}\quad y\to\infty,\end{aligned} \tag{5}$$

where $U_w(x,t)=ax/1-ct$ is the stretching sheet velocity, $V_w(x,t)=v_0/\sqrt{1-ct}$ is the mass transfer velocity, a is the initial stretching rate, c is the positive constant which measures the unsteadiness. We have $a/1-ct$ in the initial stretching rate that increases with time.

Here, the space and temperature dependent heat generation/absorption (nonuniform heat source/sink) q''' is defined as

$$q''' = \left(\frac{kU_w(x,t)}{x\upsilon}\right)\left(A^*(T_w - T_\infty) f' + B^*(T - T_\infty)\right), \tag{6}$$

where A^* and B^* are parameters of the space and temperature dependent internal heat generation/absorption. The positive and negative values of A^* and B^* represents generation and absorption, respectively.

For similarity solution, we introduce the following similarity transformation

$$\eta = \sqrt{\frac{a}{\upsilon(1-ct)}}y \ , \ \psi(x,y) = \sqrt{\frac{a\upsilon}{1-ct}}xf(\eta), \theta(\eta) = \frac{T - T_w}{T_w - T_\infty}, \phi(\eta) = \frac{C - C_w}{C_w - C_\infty},$$
$$T = T_w(x,t) = T_\infty + \frac{ax}{1-ct}\theta(\eta), \quad C = C_w(x,t) = C_\infty + \frac{ax}{1-ct}\phi(\eta), \tag{7}$$

where $\psi(x, y)$ is a stream function which satisfies the continuity equation (1) with

$$u = \frac{ax}{1-ct} f'(\eta), v = -\sqrt{\frac{a\nu}{1-ct}} f(\eta), \tag{8}$$

Using equations (6), (7) and (8), equations (2) to (4) becomes

$$f''' + ff'' - f'^2 - \frac{A}{2}\eta f'' - (A + M + K) f' = 0, \tag{9}$$

$$\theta'' + \Pr(f\theta' - f'\theta - A(\theta + \frac{1}{2}\eta\theta') + Nb\theta'\phi' + Nt\theta'^2 + Ecf''^2) + A^* f' + B^*\theta = 0, \tag{10}$$

$$Nb(\phi'' + Le(f\phi' - f'\phi - A(\phi + \frac{1}{2}\eta\phi'))) + Nt\theta'' = 0, \tag{11}$$

Subject to boundary conditions

$$f = f_w, f' = 1, \theta = 1, \phi = 1 \ at \ \eta = 0, \ f' = 0, \theta = 0, \phi = 0 \ \ as \ \eta \to \infty, \tag{12}$$

Here, $A = c/a$ is the unsteady parameter, $\Pr = \upsilon/\alpha$ is the Prandtl number,

$$Ec = U_w{}^2 / c_p(T_w - T_\infty)$$

is the Eckert number, $M = \sigma B_0{}^2 / \rho a$ is the Magnetic field parameter, $Nb = \tau D_B(C_w - C_\infty)/\upsilon$ is the Brownian motion parameter, $Nt = \tau D_T(\mathrm{T}_w - T_\infty)/\upsilon T_\infty$ is the thermophoresis parameter,

$Le = \upsilon / D_B$ is the Lewis number, $K = \upsilon / \mathrm{a}\, k_0$ is the porosity parameter and $f_w = v_0 / \sqrt{\upsilon c}$ is suction parameter.

For engineering interest the skin-friction coefficient, the reduced Nusselt number, and the reduced Sherwood numbers are given by

$$\frac{1}{2}\mathrm{Re}_x^{1/2} = f''(0), \tag{13}$$

$$\mathrm{Nu}\,\mathrm{Re}_x^{-1/2} = -\theta'(0), \tag{14}$$

$$\mathrm{Sh}\,\mathrm{Re}_x^{-1/2} = -\phi(0), \tag{15}$$

where $\mathrm{Re}_x = xU_W(x,t)/\upsilon$ is the local Reynolds number.

For steady state of the present problem we have $A = Nb = Nt = Ec = 0$. Then, closed form of the solution becomes

$$f(\eta) = \xi - \frac{1}{\xi} e^{-\xi\eta}, \tag{16}$$

$$\theta(\eta) = \frac{M(\mathrm{Pr}-1, \mathrm{Pr}+1, -\mathrm{Pr}\, e^{\xi\eta} / \xi^2)}{M(\mathrm{Pr}+1, \mathrm{Pr}-1, -\mathrm{Pr}/\xi^2)}, \tag{17}$$

where $M(d,b,z)$ denotes the confluent hyper geometric function and is given by

$$M(d,b,z) = 1 + \sum_{n=1}^{\infty} \frac{d_n z^n}{b_n n}, \tag{18}$$

$$d_n = d(d+1)(d+2)...(d+n-1),\ b_n = b(b+1)(b+2)...(b+n-1). \tag{19}$$

By using (12) equation (16) becomes

$$f(0) = f_w = \xi - \frac{1}{\xi}$$

with $\xi < 0, \xi > 0$ represents injection and suction, respectively.

3. Results and discussion

Equations (9) to (11) with the boundary conditions (12) have been solved numerically using the Shooting technique. For numerical results we consider the non-dimensional parameter values as $\mathrm{Pr} = 0.71, \mathrm{A} = 0.5, Ec = Nb = Nt = 0.1$, $K = A^* = B^* = 0.2$, $\mathrm{M} = Le = 1$ and $\eta = 2$. These values are kept constant throughout the entire study except for the varied parameters shown in the figures. The results obtained show the influences of the non-dimensional governing parameters, namely the magnetic field parameter M, the nonuniform heat generation/absorption parameter A^* *and* B^*, porosity parameter K, the thermophoresis parameter Nt, the Brownian motion parameter Nb, the unsteady parameter A and Lewis number Le on the velocity, temperature and concentration profiles. Also the friction factor, and the local Nusselt and Sherwood numbers are discussed and presented through graphs and tables.

Figure 1 shows the influence of magnetic field parameter (M) on the velocity, temperature and concentration profiles of the flow. It is evident from the figure that an increase in the magnetic field parameter causes a decline in the fluid velocity and improves the temperature and concentration profiles. It is due to the fact that an increase in magnetic field develops the force opposite to the flow, called the Lorentz force. But this force reduces the thermal and concentration boundary thickness, and so we see enhancement in the temperature and concentration profiles. Figure 2 depicts the effect of the unsteadiness parameter (A) on the velocity, temperature and concentration profiles of the flow. It is observed that an increase in unsteady parameter depreciates the temperature and concentration profiles of the flow. However, we notice a small enhancement in the velocity profiles near the boundary and afterwards by observing that the temperature and concentration profiles follow. We may explain this phenomenon as increase in unsteady parameter improves the temperature near the stretching sheet. This makes the wall temperature is higher than the ambient temperature, and due to this high wall temperature nano particles move to cooler area, causing a decline in the concentration profiles also.

Figure 3 illustrates the influence of the thermophoresis parameter (Nt) on the velocity, temperature and concentration profiles of the flow. It is clear from the figure that an increase in the thermophoresis parameter improves the temperature and concentration profiles of the flow. But it does not show any effect on the velocity profiles. Also, it is observe concentration profiles dominate the temperature profiles in this case. It may happen due to gradual enhancement in volume fraction of nanoparticles by an increase in Nt. Because of this reason we observe variation in the mass transfer rate by change in the thermophoresis parameter. Figure 4 represents the influence of the Brownian motion parameter (Nb) on the velocity, temperature and concentration profiles of the flow. It is also observed from figure that enhancement in the Brownian motion parameter increases the temperature and depreciates the concentration profiles of the flow. But there is no significant variation in the velocity profiles. Physically, this means that all nanoparticles do not have the same thermophoresis and Brownian motion values, causes an enhancement the heat transfer which in turn causes the nano particles to move away from the boundary layer, resulting in a decline of the concentration profiles.

Figure 5 reveals the effect of the porosity parameter (K) on the velocity, temperature and concentration profiles of the flow. It is evident from the figure that an increase in the porosity parameter improves both the temperature and the concentration profiles which velocity profiles show a reverse action. Generally increases in porosity parameter widen the porous layers of the flow which increases the velocity boundary layer thickness and decreases the thermal as well as concentration boundary layer thicknesses. Also, an increase in the porosity parameter releases the internal heat to the flow, which causes an enhancement of the temperature profiles. Figure 6 shows the effect of the Lewis number (Le) on the velocity, temperature and concentration profiles of the flow. It is noticed that an increase in the Lewis number depreciates the concentration profiles and a small decrement in the temperature profiles is also initially observed action that reverses after significant time. But it shows no variation in the velocity profiles. Due to this huge variation in concentration profiles the mass transfer rate is also affected.

Figures 7 and 8 depict the effect of nonuniform heat generation/absorption parameters (A^*) and (B^*) on the velocity, temperature and concentration profiles of the flow. It is clear from the figures that an increase in the heat source/sink parameters enhances the temperature and concentration profiles of the flow. But it does not show any effect on velocity profiles. It is obvious to conclude that for lesser values of A^* and B^* there is all in temperature and concentration profiles, which reveals that negative values of A^* and B^* acts like heat absorption parameters and positive values as heat generators. Figure 9 displays the effect of the Eckert number (Ec) on velocity, temperature and concentration profiles of the flow. It is observed from figure that an increase in viscous dissipation parameter increases the temperature and concentration profiles of the flow. But it is reversed in the velocity profiles. The reason behind this is an increase in Eckert number enhances the friction near velocity boundary layer and which in turn causes a reduction of the velocity profiles. But viscous dissipation improves the thermal conductivity along with concentration boundary layer. For this reason we see a hike in temperature and concentration profiles.

Table 1 shows the effect of non-dimensional governing parameters on the skin friction coefficient, the Nusselt and Sherwood numbers. It is clear from the table that an increase in the magnetic field and porosity parameters reduces the friction factor along with the heat and mass transfer rates. Increases in the unsteadiness parameter improves the skin friction coefficient, the Nusselt and Sherwood numbers. An enhancement of the thermophoresis parameter and the heat source/sink parameter depreciates the heat and mass transfer rates. A hike in the Brownian motion parameter, the viscous dissipation parameter, and the Lewis number reduces the heat transfer rate but increases the mass transfer rate. Table 2 displays the comparison of the present results with the existed before (Ishak et al. (2009) and Ferdows et al. (2014)) for checking the numerical accuracy. We have excellent agreement with earlier results.

5. Conclusions

This study reports on the boundary layer flow of a thermophoretic MHD dissipative nanofluid over an unsteady stretching sheet in a porous medium by considering space and time dependent internal heat source/sink (nonuniform heat source/sink). The governing equations are transformed in to ordinary differential equations by using similarity transformation. Numerical solutions of these equations are obtained by using the Shooting Technique. The effects of the non- dimensional governing parameters on the velocity, temperature, concentration profiles, friction factor, Nusselt and Sherwood numbers are discussed and presented through graphs and tables. Accuracy of the results is compared with that of earlier results. An excellent agreement is found between the two earlier studies.

The findings of the numerical results are summarized as follows:

(a) The thermophoresis parameter has a tendency to increase the temperature and concentration profiles and reduces the Nusselt and Sherwood numbers.
(b) The unsteadiness parameter improves the friction factor, heat and mass transfer rate.
(c) The magnetic field and porosity parameters have the capability to reduce the velocity profiles and enhance the temperature profiles. These two parameters depreciate the heat and mass transfer rate along with skin friction coefficient.
(d) The nonuniform heat source/sink parameters have a tendency to increase the temperature and concentration profiles and depreciate the heat and mass transfer rate.
(e) The Brownian motion parameter, viscous dissipation parameter and Lewis number help to enhance the mass transfer rate.
(f) The velocity profiles are not influenced by thermophoresis, Brownian motion parameters and Lewis number.

Acknowledgements

The authors wish to express their thanks to the very competent and anonymous referees for their valuable comments and suggestions. The authors from Gulbarga University acknowledge the UGC for financial support under the UGC Dr. D. S. Kothari Post-Doctoral Fellowship Scheme (No.F.4-2/2006 (BSR)/MA/13-14/0026).

REFERENCES

Afify, A.A. (2009). Similarity solution in MHD effects of thermal diffusion and diffusion thermos on free convective heat and mass transfer over a stretching surface considering suction or injection, Commum Nonlinear Sci Numer Simulat, Vol.14, pp.2204-2214.

Bachok, N., Ishak, A., Pop, I. (2010). Boundary-layer flow of nanofluids over a moving surface in a flowing fluid, Int J Therm Sci, Vol.49, 1663e1668.

Chamka, A.J., Issa, C. (2000). Effects of heat generation/absorption and thermophoresis on hydromagnetic flow with heat and mass transfer over a flat surface, Int Journal of Numerical Methods For Heat Fluid flow, Vol.10(4), pp.432-448.

Choi, S.U.S. (1995). Enhanced thermal conductivity of nanofluids with nano particles, development and applications of Newtonian flows. FED. vol.231/MD-vol.66, pp. 99-105.

Derjaguin, B.V., Yalamov, Y. (1965). Theory of thermophoresis of large aerosol particles, Journal of colloid science, Vol. 20, pp.555-570.

Dessie, H., and Kishan, N. (2014). Scaling group analysis on MHD free Convective Heat and Mass Transfer over a stretching surface with suction/injection, Heat source/sink considering viscous dissipation and chemical reaction effects, Applications and Applied Mathematics: An International Journal, Vol.9,No.2,pp.553-572.

Ece, M.C. (2005). Free convection flow about a cone under mixed thermal boundary conditions and a magnetic field, Appl Math Model, Vol. 29, pp.1121-1134.

Ferdows, M., Chapal, S.M., and Afify, A. A. (2014). Boundary Layer Flow and Heat Transfer of a Nanofluid over a Permeable Unsteady Stretching Sheet with Viscous Dissipation. Journal of Engineering Thermophysics, Vol. 23, No. 3, pp. 216–228.

Ghalambaz, M., and Noghrehabadi, A. (2014). Effects of heat generation/absorption on natural convection of nanofluids over the vertical plate embedded in a porous medium using drift-flux model, Journal of computational and applied research in mechanical engineering, Vol. 3(2), pp. 113-123.

Goren, S.L. (1977). Thermophoresis of aerosol particles in laminar boundary layer on flat plate, Journal of Colloid Interface in Science, Vol. 61, pp.77-85.

Ibrahim, F.S., Elaiw, A.M., and Bakr, A.A. (2008). Influence of viscous dissipation and radiation on unsteady MHD mixed convection flow of micropolar fluids, Appl Math Inform Sci., Vol.2, pp.143-162.

Ishak, A., Nazar, R., and Pop, I. (2009). Heat Transfer over an Unsteady Stretching Permeable Surface with Prescribed Wall Temperature, Nonlin Anal Real World Appl, Vol. 10, pp.2909–2913.

Kabir, M.A., Mahbub, M.A.L. (2012). Effects of Thermophoresis on Unsteady MHD Free Convective Heat and Mass Transfer along an inclined Porous Plate with Heat Generation in Presence of Magnetic Field. Open Journal of Fluid Dynamics, Vol. 2, pp.120-129.

Manjulatha, V., Varma, S.V.K and Raju, V.C.C. (2014). Effects of Radiation Absorption and Mass Transfer on the Free Convective Flow Passed a Vertical Flat Plate through a Porous Medium in an Aligned Magnetic Field, Applications and Applied mathematics: Aninternational jouranal,Vol.9,No.1, pp.75-93.

Mohankrishna, P., Sugunamma, V., and Sandeep, N. (2014). Radiation and magneticfield effects on unsteady natural convection flow of a nanofluid past an infinite vertical plate with heat source, Chemical and Process Engineering Research, Vol 25, pp39-52.

Noor, N.F.M., Abbansbandy, S., Hasim, I. (2013). Heat and mass transfer of thermophoretic MHD flow over an inclined radiative isothermal permeable surface in presence of heat source/sink, Int J Heat and Mass Transfer, Spl. Issue 2013, pp.1-23.

Philip, I., Shima, J.P.D., and Raj, B. (2008). Nanofluid with tunable thermal properties, Appl phys Lett, 92.043108.

Prasad, K.V., Pal, D., Umesh, V., and Rao, N.S.P. (2010). The effect of variable viscosity on MHD viscoelastic fluid flow and heat transfer over a stretching sheet, Commun Nonlinear Sci Numer Simul, Vol.15, pp.331-344.

Tsai, R. (1999). A simple approach for evaluating the effect of wall suction and thermophoresis on aerosol particle deposition from a laminar flow over a flat plate, International Communication Heat & Mass Transfer, Vol.26, pp.249–257.

Rushi Kumar, B. (2013). MHD boundary layer flow on heat and mass transfer over a stretching sheet with slip effect, Journal of Naval Architecture and Marine Engineering, Vol 10 (2), pp.16-26.

Sandeep, N., Reddy, A.V.B., Sugunamma, V. (2012). Effect of radiation and chemical reaction on transient MHD free convective flow over a vertical plate through porous media, Chemical and process engineering research, Vol. 2, pp.1-9.

Sandeep, N., Sugunamma, V., and Mohankrishna, P. (2013). Effects of radiation on an unsteady natural convective flow of a EG-Nimonic80a nanofluid past an infinite vertical plate, Advances in Physics Theories and Applications, Vol. 23, pp.36-43.

Seddeek M.A., Darwish, A.A., Abdelmeguid, M.S. (2007). Effects of Chemical Reaction and Variable Viscosity on Hydro magnetic Mixed Convection Heat and Mass Transfer for Hiemenz Flow Through Porous Media with Radiation, Commun Nonlinear Sci Numer Simulat, Vol.12, pp.195-213.

Seth, G. S., Mahto, N., Ansari, Md. S., and Nandkeolyar, R. (2010). Combined free and forced convection flow in a rotating channel with arbitrary conducting walls, Int J Eng Sci Tech, Vol. 2(5), pp.184–197.

Uddin, M.J., Beg, O.A., and Ismail, A.I. Md. (2014). Mathematical modeling of Radiative Hydro magnetic Thermosolutal Nanofluid convection slip flow in saturated porous media, Math Probs in Eng, Vol.2014, pp1-11.

Yasin, M.H.M., Arifin, N.M., Nazar, R., Ismail, F., and Pop, I. (2013). Mixed convection boundary Layer flow embedded in thermally stratified porous medium saturated by a nanofluid, Advances in Mechanical engineering, http://dx.doi.org/10.1155/2013/121943.

Table 2. Comparison of $-\theta'(0)$ values when $Nb = Nt = Ec = A^{*} = B^{*} = K = M = 0$

A	ξ	Pr	**Ishak et al. (2009)**	**Ferdows et al. (2014)**	**Present Study**
0	0.5	0.72	0.4570	0.4564	0.4566
0	0.5	1	0.5000	0.5000	0.5001
0	0.5	10	0.6452	0.6450	0.6451
0	1	0.01	0.0197	0.0191	0.0192
0	1	0.72	0.8086	0.8082	0.8082
0	1	1	1.0000	1.0000	1.0001
0	1	3	1.9237	1.9229	1.9231
0	1	10	3.7207	3.7201	3.7202
0	2	0.72	1.4944	1.4944	1.4945
0	2	1	2.0000	2.0000	2.0001
0	2	10	16.0842	16.0835	16.0837
1	0.5	1	0.8095	0.8086	0.8087
1	1	1	1.3205	1.3201	1.3203
1	2	1	2.2224	2.2219	2.2221

Table 1. Values of $f''(0), -\theta'(0)$ and $-\phi'(0)$ for different values of $M, Nt, Nb, Ec, Le, A, A^*$, B^* *and* K when $\Pr = 0.71$

M	Nt	Nb	Ec	A	A^*	B^*	Le	K	$f''(0)$	$-\theta'(0)$	$-\phi'(0)$
0.5	0.1	0.1	0.1	0.5	0.2	0.2	1	0.2	-1.483240	0.663728	0.445664
1.0	0.1	0.1	0.1	0.5	0.2	0.2	1	0.2	-1.643168	0.642061	0.437007
1.5	0.1	0.1	0.1	0.5	0.2	0.2	1	0.2	-1.788854	0.623223	0.430248
1.0	**0.1**	0.1	0.1	0.5	0.2	0.2	1	0.2	-1.643168	0.642061	0.437007
1.0	**0.2**	0.1	0.1	0.5	0.2	0.2	1	0.2	-1.643168	0.635688	-0.292302
1.0	**0.3**	0.1	0.1	0.5	0.2	0.2	1	0.2	-1.643168	0.629627	-1.020032
1.0	0.1	**0.1**	0.1	0.5	0.2	0.2	1	0.2	-1.643168	0.642061	0.437007
1.0	0.1	**0.2**	0.1	0.5	0.2	0.2	1	0.2	-1.643168	0.620969	0.809749
1.0	0.1	**0.3**	0.1	0.5	0.2	0.2	1	0.2	-1.643168	0.600568	0.933795
1.0	0.1	0.1	**0**	0.5	0.2	0.2	1	0.2	-1.643168	0.690198	0.399498
1.0	0.1	0.1	**0.4**	0.5	0.2	0.2	1	0.2	-1.643168	0.497588	0.549595
1.0	0.1	0.1	**0.8**	0.5	0.2	0.2	1	0.2	-1.643168	0.304784	0.699859
1.0	0.1	0.1	0.1	**0.1**	0.2	0.2	1	0.2	-1.729706	0.454755	0.171272
1.0	0.1	0.1	0.1	**0.2**	0.2	0.2	1	0.2	-1.706438	0.533013	0.278271
1.0	0.1	0.1	0.1	**0.3**	0.2	0.2	1	0.2	-1.684298	0.580719	0.346506
1.0	0.1	0.1	0.1	0.5	**0.1**	0.2	1	0.2	-1.643168	0.685642	0.488368
1.0	0.1	0.1	0.1	0.5	**0.2**	0.2	1	0.2	-1.643168	0.642061	0.437007
1.0	0.1	0.1	0.1	0.5	**0.3**	0.2	1	0.2	-1.643168	0.598366	0.385736
1.0	0.1	0.1	0.1	0.5	0.2	**0.1**	1	0.2	-1.643168	0.720154	0.536374
1.0	0.1	0.1	0.1	0.5	0.2	**0.2**	1	0.2	-1.643168	0.642061	0.437007
1.0	0.1	0.1	0.1	0.5	0.2	**0.3**	1	0.2	-1.643168	0.545292	0.312183
1.0	0.1	0.1	0.1	0.5	0.2	0.2	**1**	0.2	-1.643168	0.642061	0.437007
1.0	0.1	0.1	0.1	0.5	0.2	0.2	**2**	0.2	-1.643168	0.634483	1.157496
1.0	0.1	0.1	0.1	0.5	0.2	0.2	**3**	0.2	-1.643168	0.630564	1.686328
1.0	0.1	0.1	0.1	0.5	0.2	0.2	1	**0.5**	-1.732051	0.630465	0.432758
1.0	0.1	0.1	0.1	0.5	0.2	0.2	1	**1.0**	-1.870829	0.613002	0.426899
1.0	0.1	0.1	0.1	0.5	0.2	0.2	1	**1.5**	-2.000000	0.597438	0.422251

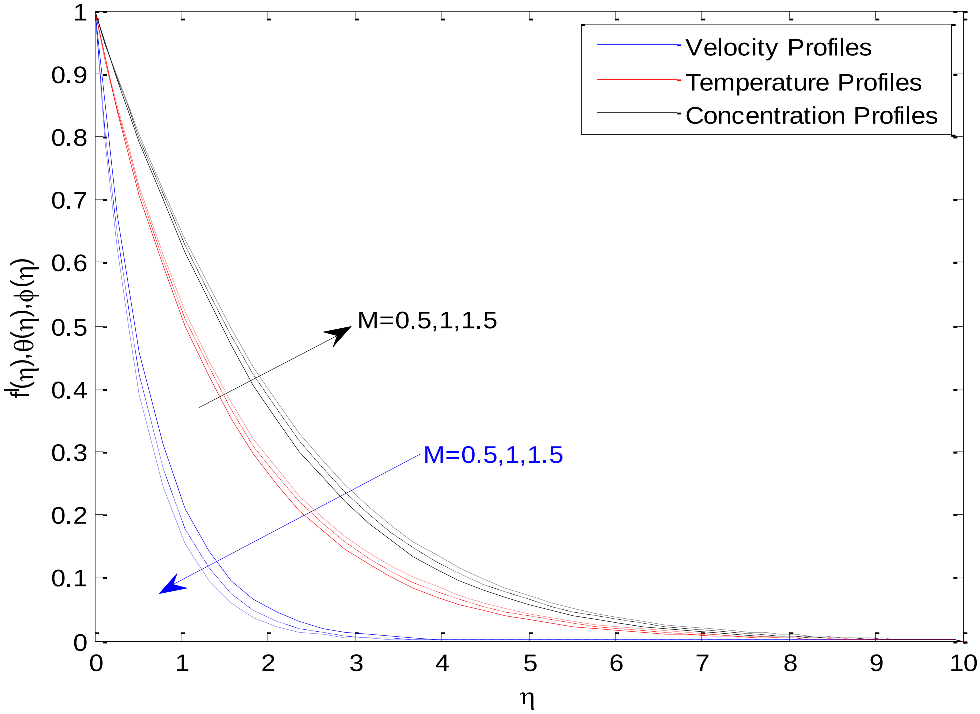

Figure.1. Velocity, temperature and concentration profiles for various values of Magnetic field parameter (M)

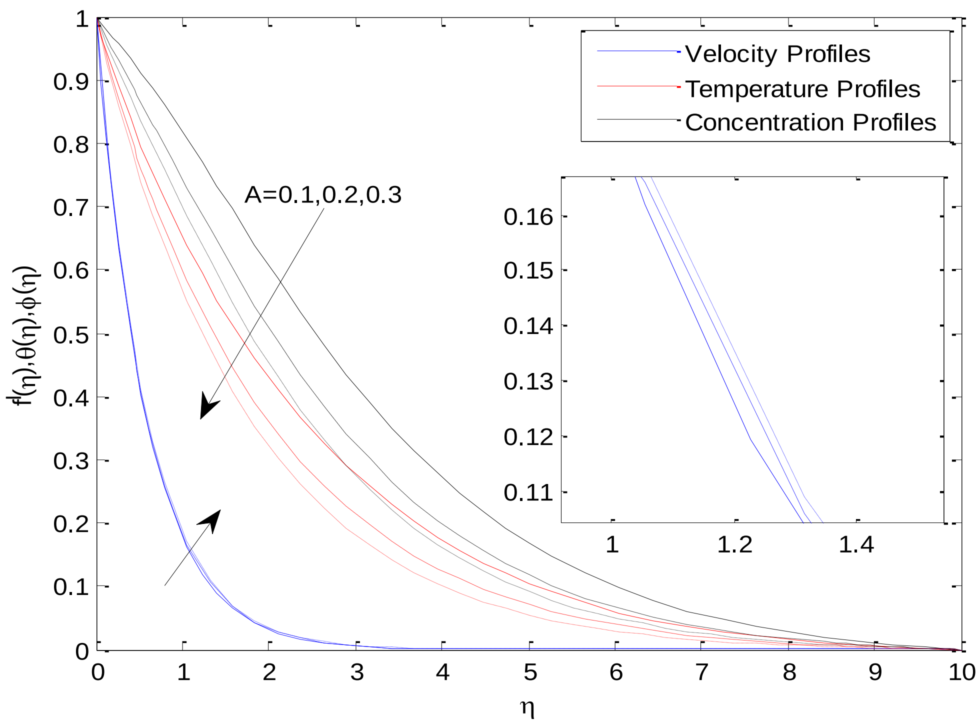

Figure.2. Velocity, temperature and concentration profiles for various values of Unsteadiness parameter (A)

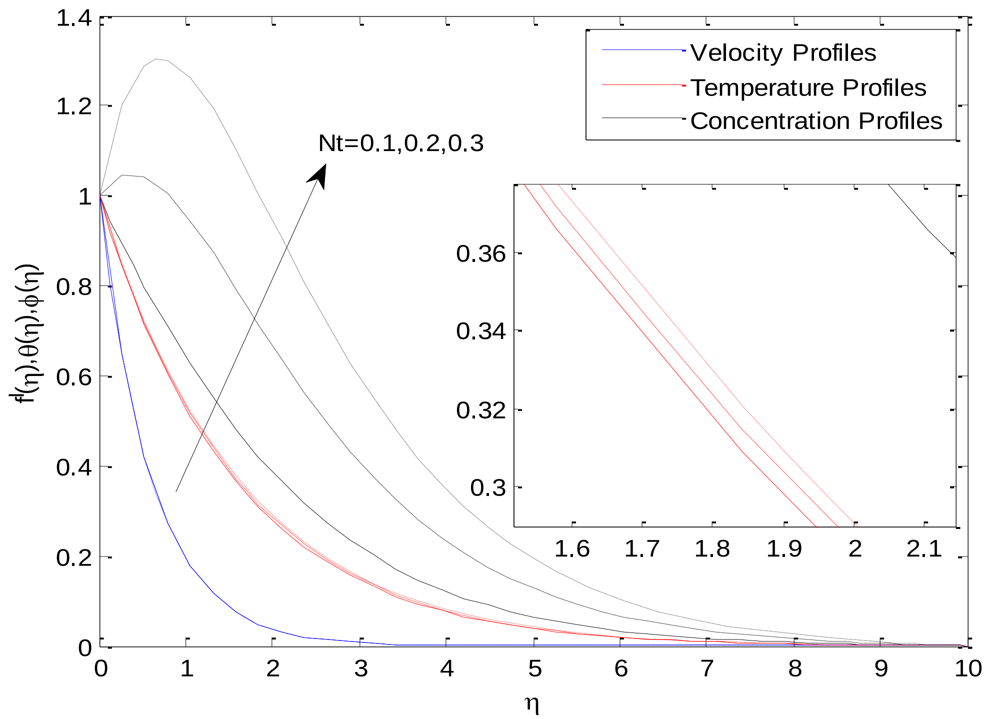

Figure.3. Velocity, temperature and concentration profiles for various values of Thermophoresis parameter (Nt)

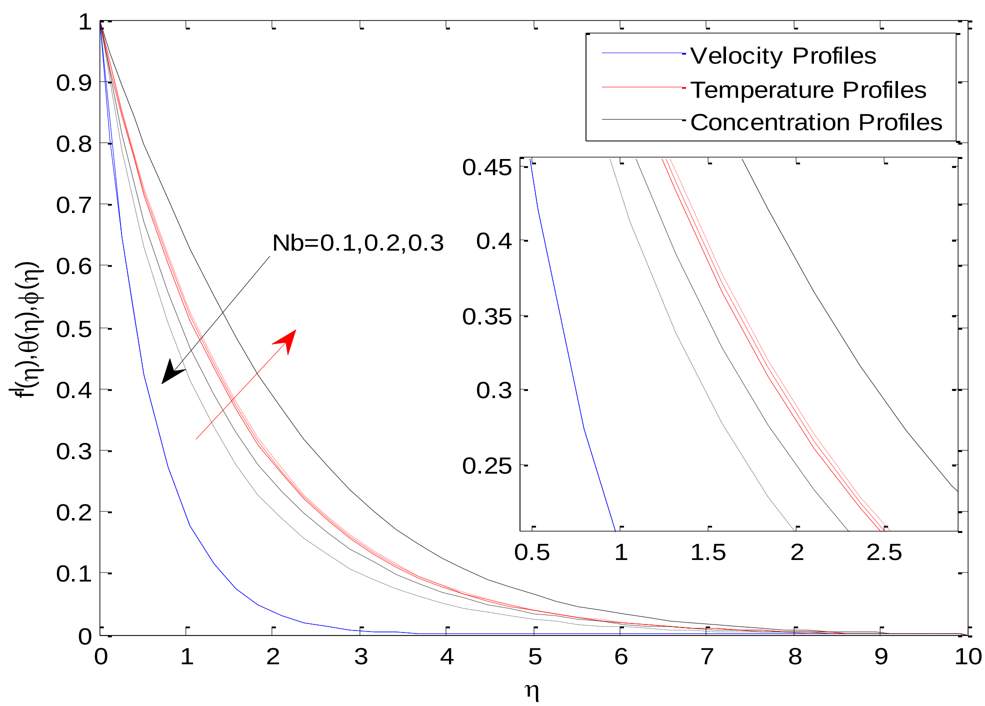

Figure.4. Velocity, temperature and concentration profiles for various values of Brownian motion parameter (Nb)

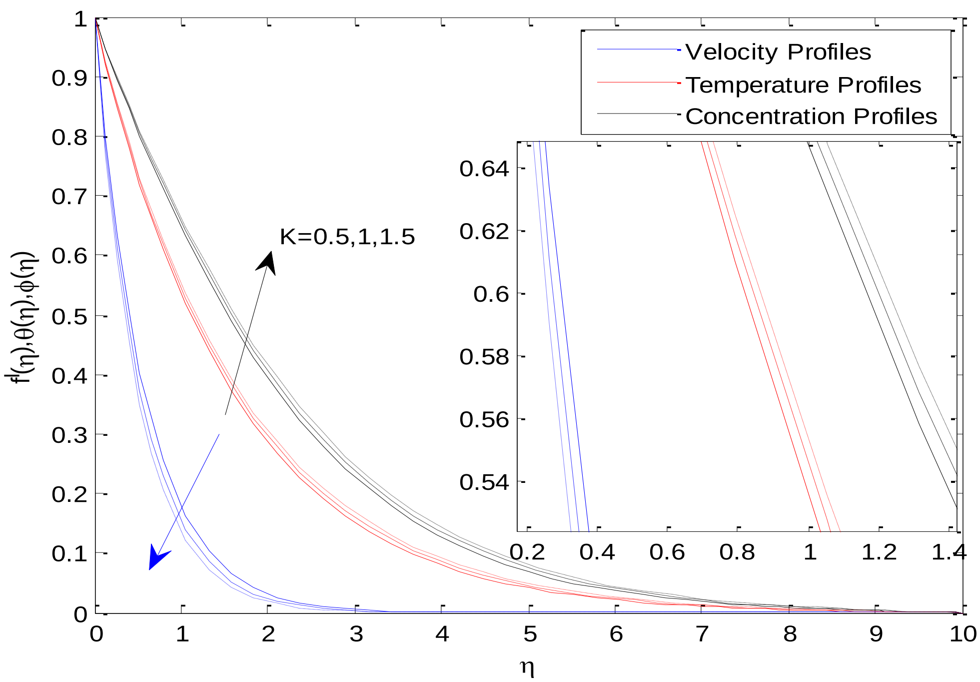

Figure.5. Velocity, temperature and concentration profiles for various values of Porosity parameter (K)

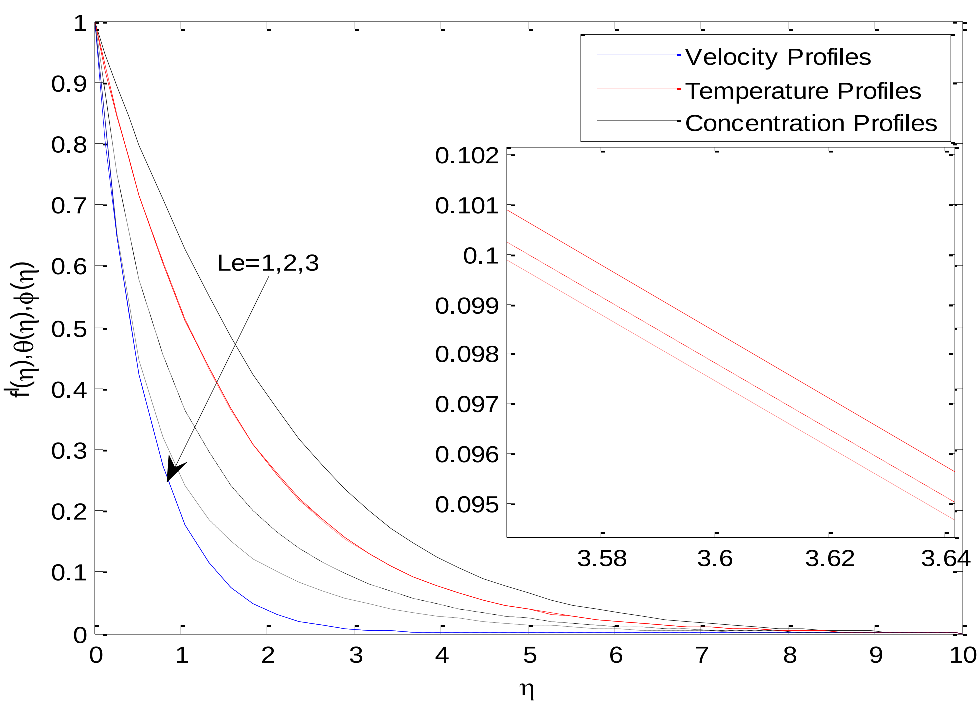

Figure 6. Velocity, temperature and concentration profiles for various values of Lewis number (Le)

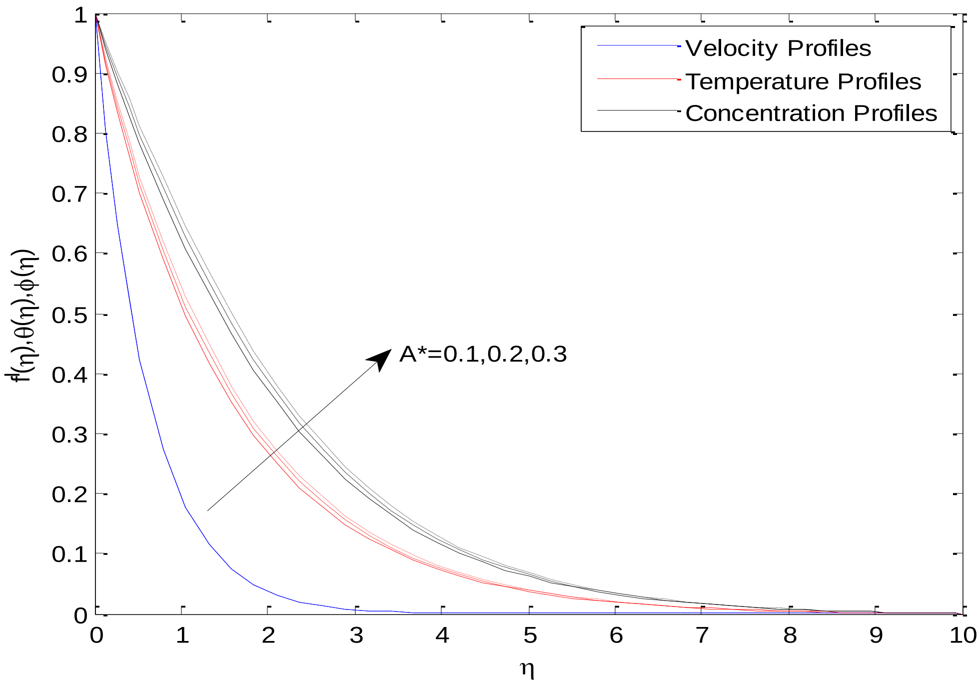

Figure.7. Velocity, temperature and concentration profiles for various values of Heat source/sink parameter (A^*)

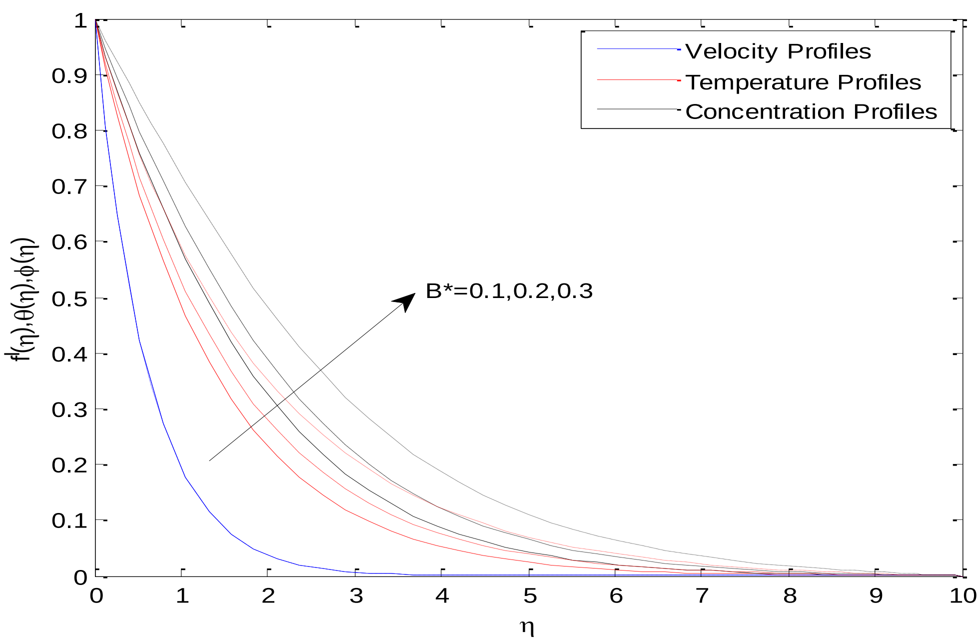

Figure.8. Velocity, temperature and concentration profiles for various values of Heat source/sink parameter (B^*)

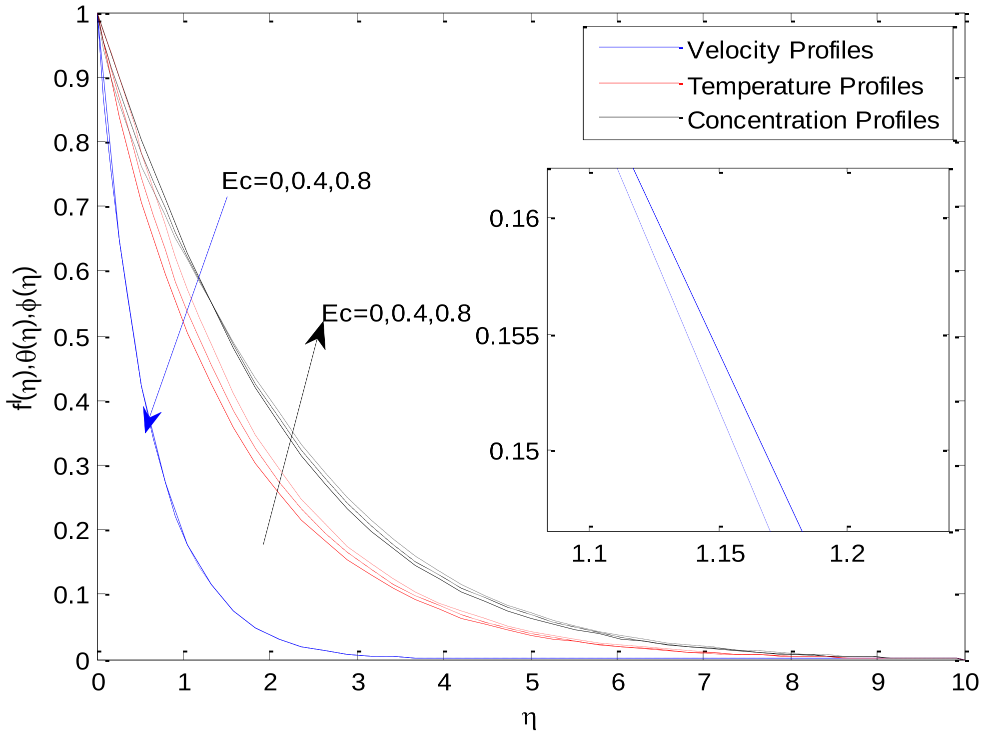

Figure.9. Velocity, temperature and concentration profiles for various values of Viscous dissipation parameter (Ec)